

BSC Downtube Structure Mechanical Design and Analysis

Bernie Weinstein & Eric Ponslet

September 13, 1996

Revision *a*, January 14, 1997

Abstract

A final analytical design for the downtube is developed. This technical note traces the evolution of the design from an earlier two piece version to the current one piece design. The final design is checked against requirements for natural frequencies, thermal noise response, and static stresses.

Table of Contents

1. Introduction.....	3
2. Design Requirements	3
2.1 Response to Residual Seismic Noise.....	3
2.2 Response to Thermal Noise	4
2.3 Static Stresses due to Gravity Loads	5
3. Analysis	5
4. History	6
4.1 Two Piece Downtube Configuration.....	6
4.2 One Piece Configuration.....	8
5. Description of Current Design	8
6. Performance	9
6.1 Natural Modes	9
6.2 Thermal Noise Evaluation	11
6.3 Static Stresses.....	12
7. References	12
8. Appendix A: Effect of mesh density and element order on frequency analysis	14

1. Introduction

This notes roughly traces the development of the mechanical components of the downtube structure for the BSC isolation stacks. The stack provides shielding from floor-borne seismic vibrations. It is composed of 4 stages of soft springs and “rigid” bodies arranged symmetrically in a 4-leg configuration^[1]. The stack is resting on a support platform and supports the large downtube structure that connects the top of the stack legs to the optics table situated below the support platform^[1].

To maintain isolation performance at “high” frequencies (above 40 Hz), it is crucial to guarantee that resonances in any of the stack components (the “rigid” bodies and the springs) have sufficiently high frequencies and low Q so they do not produce violations of the isolation requirements. This can be guaranteed by imposing a lower limit on the natural frequencies; this limit is defined by looking at isolation requirements and expected stack performance, with assumptions on the quality factor of the structures involved (see next section).

In addition, thermal noise internally excites the natural modes of the downtube structure. Maintaining resonant response to thermal noise below the displacement noise targets implies upper limits on the quality factor (Q) of the downtube modes as a function of the natural frequencies and effective masses of those modes as described in Section 2.1.

Resonances in the springs and support structure are considered elsewhere^[2,3]. The other components of the stack (leg elements and downtube structure) are designed as light weight, high stiffness structures as described in this note. Note that we do not present results on the natural frequencies of the leg elements (solid stainless steel discs, 540 mm in diameter and various thicknesses). Simple analysis shows that a 540 mm diameter by 50 mm thick stainless steel disc has no resonant frequency below 840Hz. This shows that resonances in the leg elements are not a concern.

2. Design Requirements

We were initially advised to design all stack components for fundamental frequencies above 500Hz. This value was based on rough expectations of stack performance and component masses. The initial design efforts attempted to achieve that goal (see Section 3).

As soon as design requirements^[4] and preliminary stack designs^[1] became available, we were able to formulate more explicit requirements for the frequencies and quality factors of the modes of the downtube structure. These requirements are based on limiting the response of the downtube to residual seismic noise on one hand and internal thermal noise on the other.

2.1 Response to Residual Seismic Noise

Figure 1 shows the isolation requirements for the BSC stacks^[4], compared to the expected performance of isolation stacks using Viton springs^[5] (worst case since the performance of metal spring stacks is far superior).

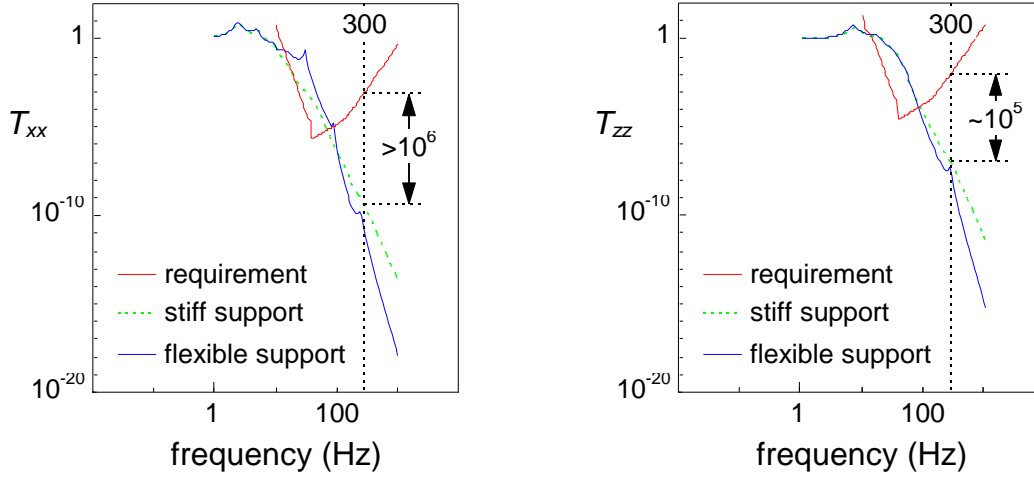


Figure 1: expected isolation performance with 4-stage Viton stack^[9] (performance with metal springs is better); predictions with and without simulated flexibility of the support structure are shown.

The figure shows that if we conservatively assume that the quality factor (Q) of the leg elements and downtube structure will not exceed 10^4 (i.e. 0.01% loss factor), a lower limit of 300Hz on the natural frequencies of the stack components provides at least a factor 10 safety factor w.r.t. the requirements.

2.2 Response to Thermal Noise

The motion of the suspension point on the optics table due to thermal noise excitation of mode $\#i$ is given as^[4]

$$X_{SUS,i} = \sqrt{\frac{4k_B T Q_i}{m_i (2\pi f_i)^3}}, \quad (1)$$

where k_B is Boltzmann's constant, T the downtube temperature in °K, and f_i , Q_i , and m_i are the natural frequency (Hz), quality factor, and effective mass at the attachment point of the SUS of the i^{th} mode, respectively.

This motion is attenuated by the SUS pendulum to result in test mass motion along the X axis equal to

$$X_{MASS,i} = X_{SUS,i} \cdot T_{xx}^{SUS}(f_i), \quad (2)$$

where $T_{xx}^{SUS}(f_i)$ is the horizontal transmissibility of the SUS pendulum, evaluated at f_i . The test mass motion $X_{MASS,i}$ is to remain a factor 20 (10×2 for two test masses) below the initial noise target X_{target} . This leads to the following expression for the maximum allowable Q_i for a mode of the downtube structure with frequency f_i and effective mass m_i :

$$Q_i \leq Q_i^{\max} = 3.8293 \times 10^{19} \cdot \left| \frac{X_{target}}{T_{xx}^{SUS}} \right|_{f_i}^2 \cdot m_i \cdot f_i^3. \quad (3)$$

Figure 2 shows these limit values as a function of f and m . This requirement will be evaluated a posteriori for the lowest modes of candidate designs.

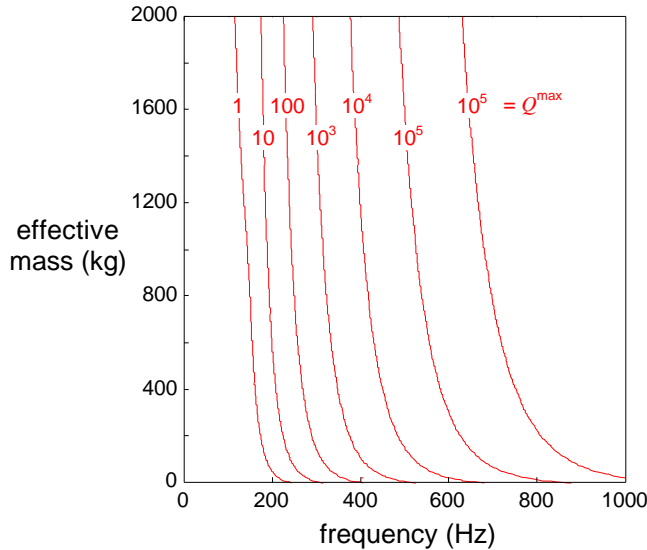


Figure 2: Thermal noise requirements on resonances of downtube structure; the chart gives minimum acceptable value of Q at resonance as a function of natural frequency and effective mass of resonant mode (normalized to unit resultant motion at SUS attachment point).

Note that similar reasoning can be applied for the coupling terms $T_{xz}^{SUS}(f_i)$ and $T_{xc}^{SUS}(f_i)$, leading to different limits on the Q 's. All modes must be checked against all limits.

2.3 Static Stresses due to Gravity Loads

Since the structure is designed for high natural frequencies, the static stresses are expected to be very low. Finite element calculations are used for verifications on final designs.

3. Analysis

Both the downtube and the leg elements are supported by soft springs (viton, coil or, leaf). The natural frequencies associated with these springs (stack component oscillating as a rigid body on the springs) range from about 2 to 30 Hz, a factor 10 below the 300 Hz structural design goal. This decouples the dynamic behavior of the stack components from their supports, essentially simulating free-free boundary conditions. Because of this, all modal analysis reported in this document were performed in free-free conditions.

The downtube structure is analyzed with finite elements (COSMOS), using shell elements. In all cases, the entire outer (bottom) face of the optics table is given an artificially high density to simulate a payload of 227 kg (500 lbs) uniformly smeared on the optics table.

4. History

4.1 Two Piece Downtube Configuration

Following numerous design approaches, the design presented at the April 04, 1996 Caltech/Hytec meeting^[5] consisted of a downtube and optics table, a cross made of square tubing, and a large upper ring, as seen in Fig. 3. Our requirement, at that time, was to design structures without resonances below 500 Hz..

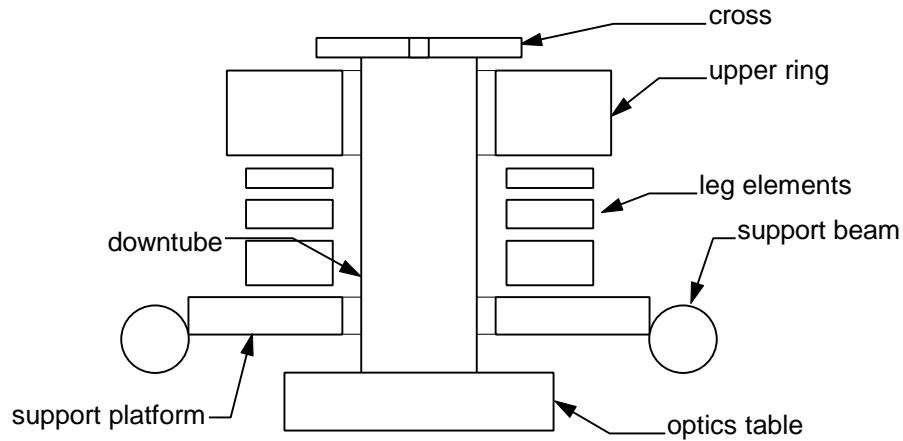


Figure 3: previous design configuration^[6]

The structure is made entirely of aluminum. The small cross at the top of the downtube is resting on a large upper ring through an additional layer of springs. This upper ring consists of a large welded sandwich aluminum structure. After a number of iterations we settled on the following dimensions: two 25.4 mm (1") thick faces plates separated by a core with an almost square web grid (core pitch varies from 90 mm (3.5") to 120 mm (4.7")), built with aluminum plates 3.175 mm (.125") thick, and closed by inner and outer rings 12.7 mm (.5") thick. The core height is 343 (13.5"). The finite element model of the ring is shown in Fig. 4.

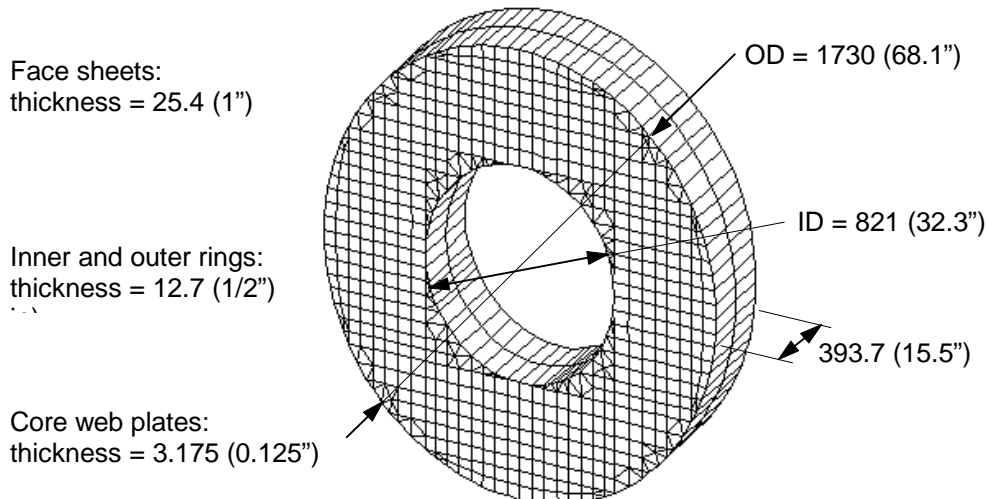


Figure 4: upper ring geometry; all dimensions in mm (inches).

Resonances for this design occur at 425, 434, and 509 Hz. (See Fig. 5). These high resonant frequencies were achieved after many iterations in which the face plate separation and thickness, core spacing and thickness, as well as the thicknesses of the inner and outer closure rings were varied.

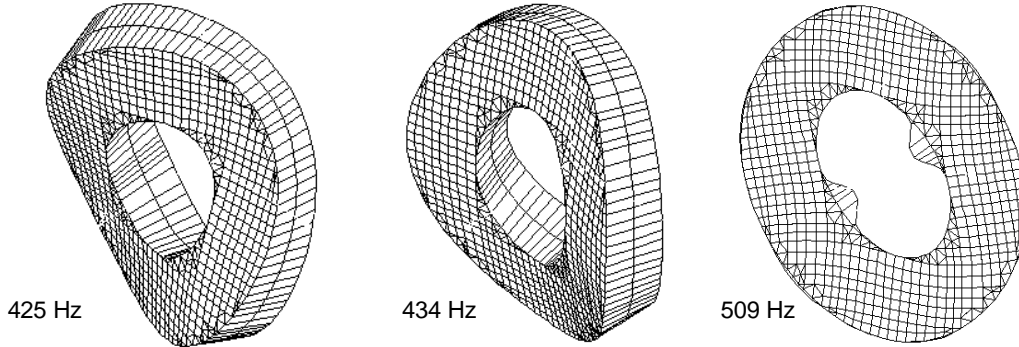


Figure 5: upper ring resonances.

The downtube portion of the same design is shown in Fig. 6. In addition to manipulating optics table variables (core grid, depth, and web thickness, face plate thickness, closure rings), the downtube material thickness, stiffening ring spacing, thickness and depth were also varied. In the final design, the optics table is a hollow core structure, with 4 internal stiffening rings and a number of radial stiffeners made of 6.35 mm (.25") material. Both face plates are 12.7 mm (.5") thick. The downtube itself is rolled from 19.05 mm (.75") aluminum and seam welded. In addition to the end stiffener, visible in Fig. 6, there are 3 regularly spaced internal stiffening rings, also 19.05 mm (.75") thick.

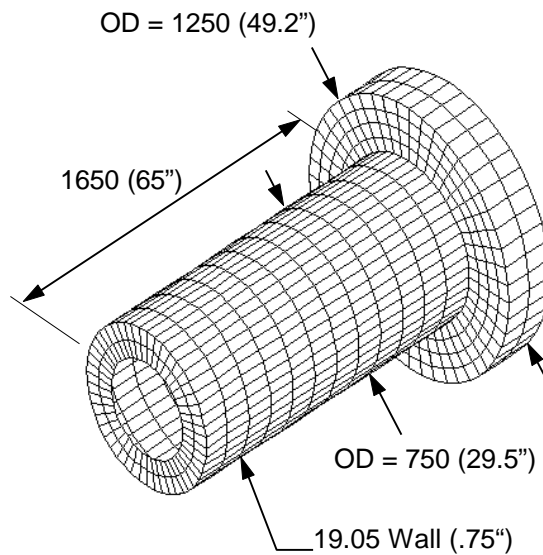


Figure 6: previous downtube.

The first three downtube resonances occur at frequencies of 430, 462, and 536 Hz. (for simplicity, the cross was not modeled). The corresponding mode shapes are shown in Fig. 7.

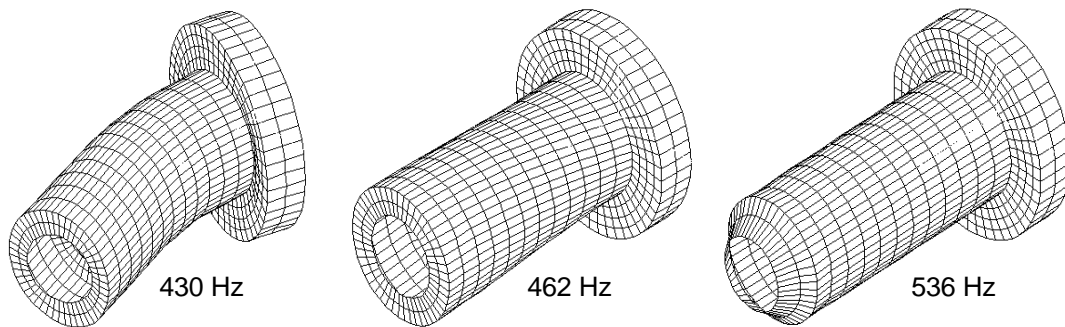


Figure 7: downtube resonances.

4.2 One Piece Configuration

Subsequent analyses (see section 2.1) determined that structures with resonances above 300 Hz (not 500) would satisfy isolation requirements. The present design (Fig. 8) eliminates the large upper ring and utilizes a simple cross beam for interfacing with the leg elements. The elimination of the upper ring led to a the shorter downtube, with thinner wall and fewer stiffening rings.

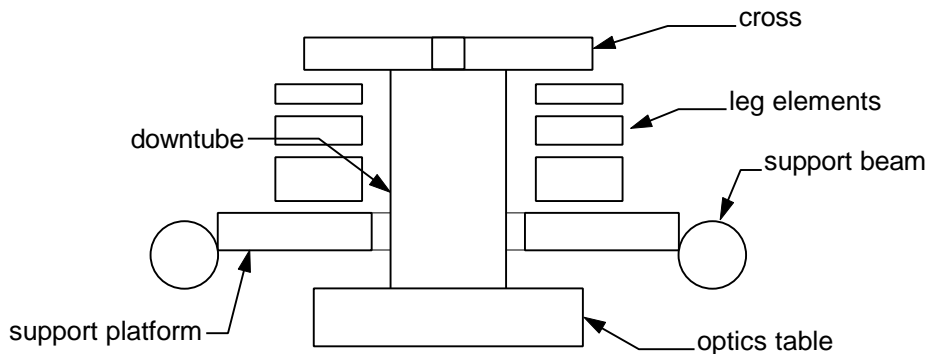


Figure 8: present design.

The 2-piece design utilized a hollow core ring weighing 990 pounds, plus a downtube that weighed 950 pounds, for a total of 1,940 pounds, not including the cross. This one-piece design weighs only 830 pounds, and eliminates the need for the costly large ring. (Vendor supplied budgetary cost estimates indicated that 15 rings would have cost \$25k each).

5. Description of Current Design

Figure 9 shows the final configuration of the downtube. The optics table is a honeycomb construction, with 4 internal stiffening rings and a pattern of radial stiffeners, spaced to maintain a maximum allowable unsupported faceplate area. In other words,

there are more radial stiffeners near the perimeter of the optics table than there are in its center. The downtube is rolled from 5/8" aluminum and seam welded. It has 2 internal stiffening rings. Square slots are cut into the end of the downtube, and the cross, made from 8" x 1/2" square tubing, is fitted there and welded.

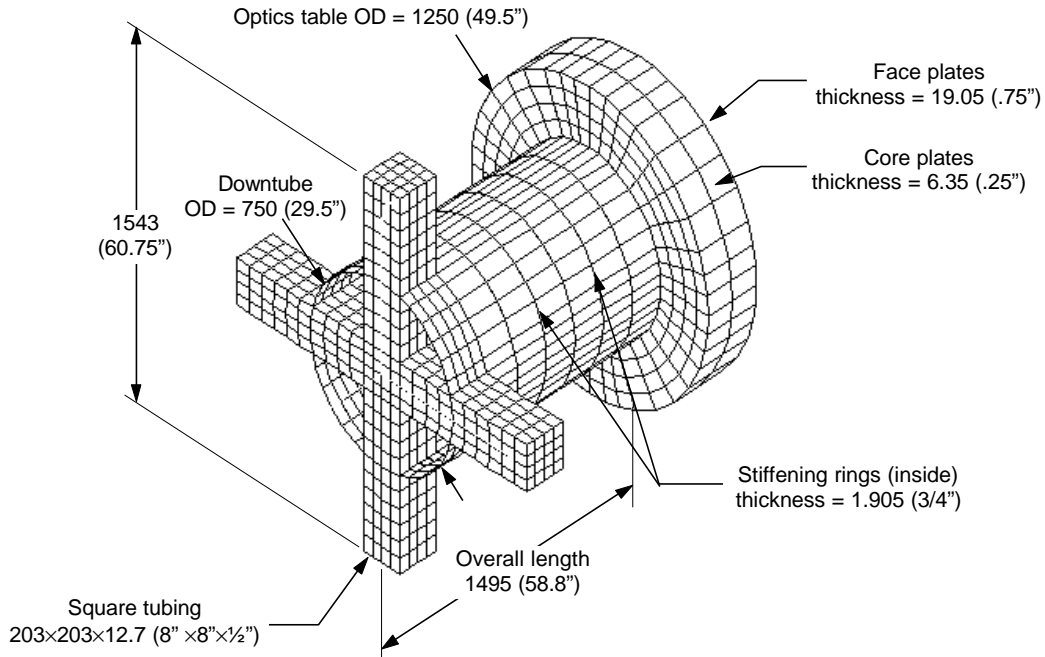


Figure 9: present design geometry; all dimensions in mm (inches)

6. Performance

6.1 Natural Modes*

The first natural frequency is 349 hertz, comfortably above the requirements of the system. Higher modes occur at 354, 370, 371, 399, and 421 Hz (Fig. 10). Note that we initially had more structure around the cross/downtube interface, and were rewarded with higher resonances. However, by setting the cross beams into the downtube, we reduced the manufacturing complexity while achieving acceptable performance.

* Rev a note: analysis reflects earlier design (09/13/96). Downtube has been lengthened and optics table bottom plate thickened, which should lower frequencies by a few percent.

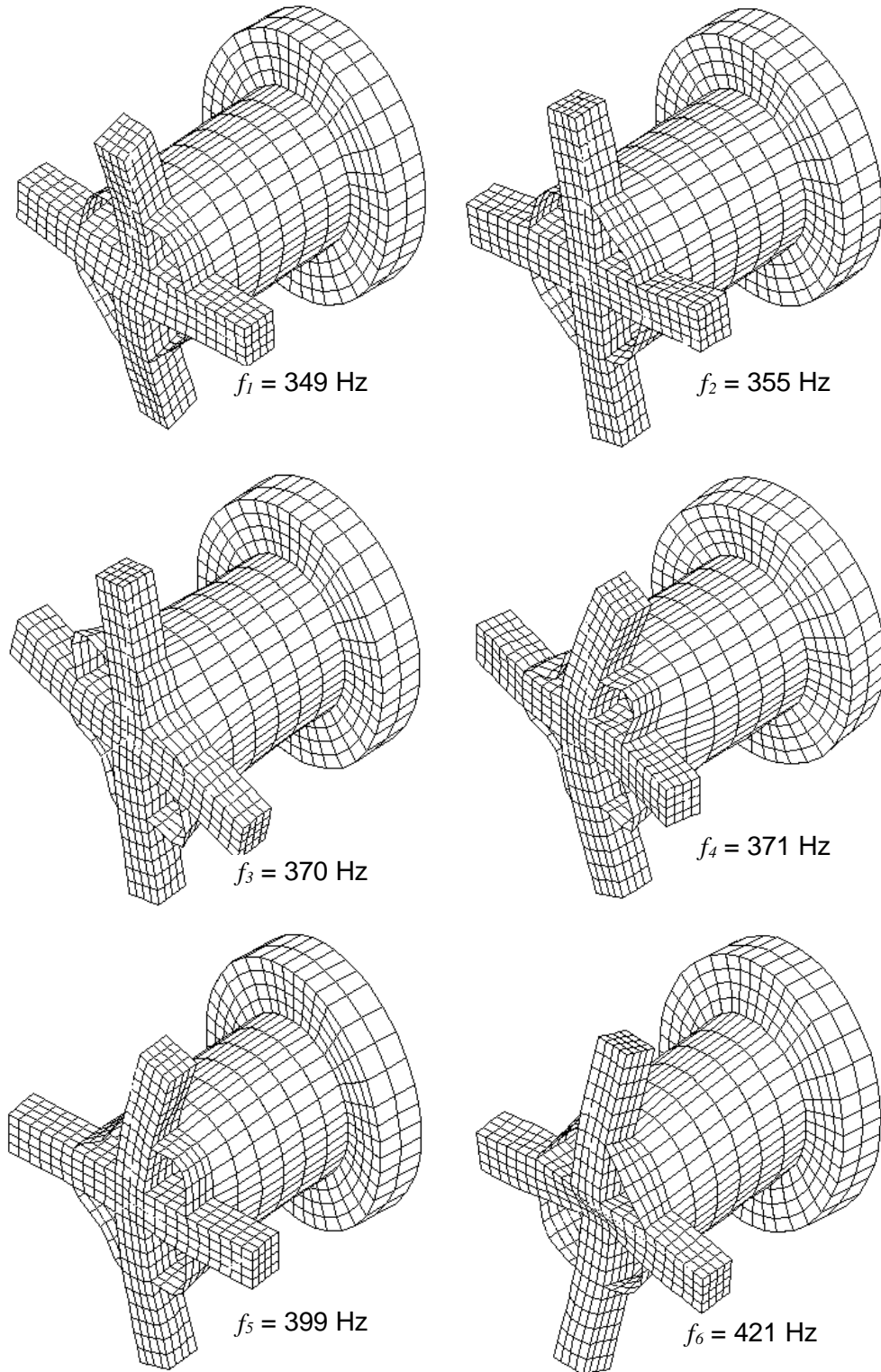


Figure 10: First 6 resonant modes.

Note that the results of Fig. 10 were obtained using 8 node shell elements, while all preliminary work was done with 4 node elements. The lowest frequency observed in

the latter model was 371 Hz. Changing to the more accurate 8 node elements reduced the first natural frequency to 349 Hz., a 6% reduction. Run time for the simpler model was about 90 minutes, while a similar calculation with 8 node elements took 8 hours. In the course of this analysis, a study was made of the effect of element density and element order on the accuracy of the prediction of resonances. The results are contained in appendix A.

6.2 Thermal Noise Evaluation**

Free-free natural modes obtained from NASTRAN runs were used to evaluate effective masses m_i at the center of the optics table: the mode shapes \mathbf{f}_i are first normalized to unit horizontal amplitude (resultant of two horizontal components) or vertical amplitude or rotation around the vertical axis at the optics table centerpoint, then used to evaluate the modal masses of the lowest few modes ($m_i = \mathbf{f}_i^T \mathbf{M} \mathbf{f}_i$, where \mathbf{M} is the mass matrix of the downtube and payload). Using equation 3 (and similar expressions for the coupling terms, see Section 2.2), maximum allowable Q 's are estimated for each mode as listed in Table 1.

mode i	f_i (Hz)	T_{xx}		T_{xz}		T_{xc}	
		m_i (kg)	Q_i^{max}	m_i (kg)	Q_i^{max}	m_i (kg)	Q_i^{max}
1	349	43158.	106210.	$1.21 \cdot 10^{16}$	$6.44 \cdot 10^{18}$	$1.28 \cdot 10^{15}$	$1.54 \cdot 10^{20}$
2	355	$2.54 \cdot 10^{14}$	$7.14 \cdot 10^{14}$	$2.41 \cdot 10^{16}$	$1.46 \cdot 10^{19}$	329.	$4.50 \cdot 10^7$
3	370	$2.48 \cdot 10^{12}$	$1.02 \cdot 10^{13}$	$2.55 \cdot 10^{18}$	$2.26 \cdot 10^{21}$	13411.	$2.68 \cdot 10^9$
4	371	380010.	$1.62 \cdot 10^6$	$1.99 \cdot 10^{15}$	$1.83 \cdot 10^{18}$	$6.33 \cdot 10^{10}$	$1.31 \cdot 10^{16}$
5	399	$1.84 \cdot 10^7$	$1.48 \cdot 10^8$	$7.26 \cdot 10^{15}$	$1.26 \cdot 10^{19}$	$9.16 \cdot 10^{11}$	$3.59 \cdot 10^{17}$
6	421	23108.	302910.	$3.98 \cdot 10^{14}$	$1.13 \cdot 10^{18}$	$7.48 \cdot 10^{11}$	$4.77 \cdot 10^{17}$
7	441	251050	$4.99 \cdot 10^6$	$1.06 \cdot 10^{16}$	$4.55 \cdot 10^{19}$	$2.08 \cdot 10^{14}$	$2.02 \cdot 10^{20}$
8	462	$2.60 \cdot 10^{14}$	$7.93 \cdot 10^{15}$	6003.	$3.95 \cdot 10^7$	$1.23 \cdot 10^{13}$	$1.82 \cdot 10^{19}$
9	463	10024.	308350.	$3.31 \cdot 10^{10}$	$2.20 \cdot 10^{14}$	$1.69 \cdot 10^{14}$	$2.53 \cdot 10^{20}$
10	478	$1.0578 \cdot 10^{15}$	$4.34 \cdot 10^{16}$	218870.	$1.94 \cdot 10^9$	$1.25 \cdot 10^{14}$	$2.49 \cdot 10^{20}$
11	556	$6.4461 \cdot 10^{11}$	$1.05 \cdot 10^{14}$	$1.48 \cdot 10^{12}$	$5.20 \cdot 10^{16}$	$1.08 \cdot 10^9$	$8.49 \cdot 10^{15}$
12	560	$2.4382 \cdot 10^{12}$	$4.17 \cdot 10^{14}$	$4.87 \cdot 10^9$	$1.79 \cdot 10^{14}$	$2.54 \cdot 10^{13}$	$2.12 \cdot 10^{20}$
13	583	$1.6679 \cdot 10^{13}$	$4.15 \cdot 10^{15}$	639.	$3.44 \cdot 10^7$	$9.51 \cdot 10^{10}$	$1.15 \cdot 10^{18}$
14	611	$1.5441 \cdot 10^{13}$	$5.81 \cdot 10^{15}$	167.	$1.36 \cdot 10^7$	$5.68 \cdot 10^{10}$	$1.04 \cdot 10^{18}$
15	615	$9.9738 \cdot 10^{13}$	$3.98 \cdot 10^{16}$	514.	$4.42 \cdot 10^7$	$1.89 \cdot 10^{11}$	$3.68 \cdot 10^{18}$
16	683	29309.	$3.02 \cdot 10^8$	$6.99 \cdot 10^{11}$	$1.56 \cdot 10^{17}$	$6.76 \cdot 10^{11}$	$3.39 \cdot 10^{19}$
17	690	73287.	$8.16 \cdot 10^7$	$1.05 \cdot 10^{11}$	$2.53 \cdot 10^{16}$	$1.48 \cdot 10^{12}$	$8.01 \cdot 10^{19}$
18	702	$1.08 \cdot 10^6$	$1.42 \cdot 10^9$	$3.29 \cdot 10^{13}$	$9.30 \cdot 10^{18}$	$3.46 \cdot 10^{13}$	$2.21 \cdot 10^{21}$

Table 1: maximum allowable downtube Q 's for thermal noise response. Limits are given based on direct horizontal, vertical-horizontal, and yaw-horizontal couplings in the SUS. Limit Q 's below 10^6 are highlighted.

First note that most modes listed in the table have very large effective masses at the optics table centerpoint. This is because those modes have very small amplitudes at the centerpoint of the optics table. Almost all modes listed only involve the upper cross; two modes (11 and 12) involve the optics table.

** Rev a note: analysis reflects earlier design (09/13/96). Downtube has been lengthened and optics table bottom plate thickened, which should lower frequencies by a few percent. Q requirements are not expected to change significantly.

The lowest of all Q requirements applies to direct horizontal coupling with the first elastic mode and is about 10^5 (0.001% loss factor), which is well above typical Q 's for large welded structures (100-500) or even material damping at nanostrain level in solid aluminum (400-8400^[8]).

6.3 Static Stresses

As expected, stresses due to gravity loads are extremely low. In the analysis, two elements (13 nodes) in each leg are supported in the vertical direction. Maximum nodal stress is 720 psi (Fig. 11), with 500 pounds of payload added to the optics table.

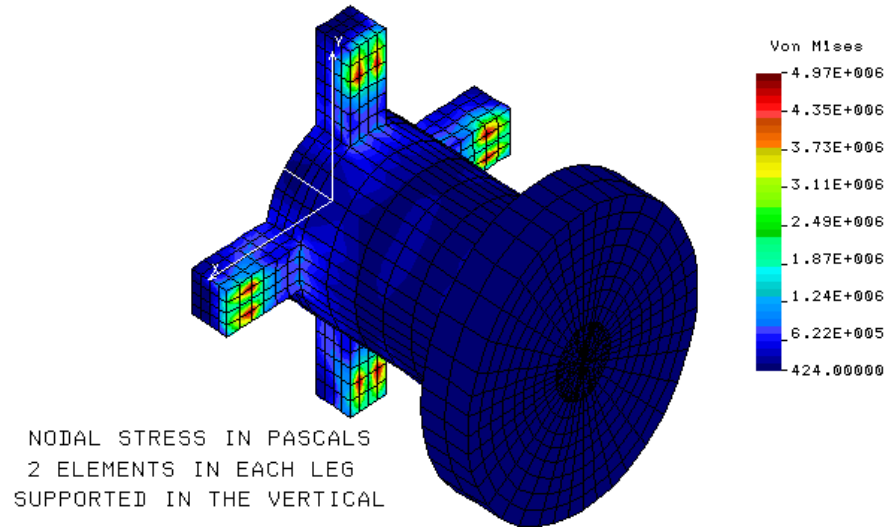


Figure 11: Nodal Von Mises stress due to gravity.

7. References

1. E. Ponslet, "BSC Stack Design - Trend Study," HYTEC-TN-LIGO-03, March 1st, 1996.
2. E. Ponslet, "Design of Vacuum Compatible Damped Metal Springs for Passive Vibration Isolation of the LIGO Detectors," HYTEC-TN-LIGO-04, July 10, 1996.
3. B. Weinstein and E. Ponslet, "Design of BSC Stack Support Structure," HYTEC-TN-LIGO-06, to be released.
4. F. Raab and N. Solomonson, "Seismic Isolation Design Requirements Document" (draft and early corrections), LIGO draft document LIGO-T960065-02-D, California Institute of Technology and Massachusetts Institute of Technology, April 15, 1996.
5. Ponslet, "BSC Seismic Isolation - Projected Performance Update," HYTEC-TN-LIGO-07, to be released.
6. W. O. Miller and E. Ponslet, Caltech/Hytec meeting, presentation slides, April 04, 1996.
7. R. Blevins, *Formulas for Natural Frequency and Mode Shape*, 1995 edition, pp. 253-261.

8. J. M. Ting and E. F. Crawley, "Characterization of Damping of Materials and Structures from Nanostrain Levels to One Thousand Microstrain," *AIAA Journal*, Vol. **30**, No. 7, July 1992.

8. Appendix A: Effect of mesh density and element order on frequency analysis

The study considers a 20" x 20" x 1/2" 6061 aluminum plate with all edges free, supported, and clamped.

Analytical values^[7]

mode	1	2	3	4	5
free-free	164	240	296	424	424
supported	235	598	598	957	1196
clamped	436	890	890	1313	1595

Values obtained from COSMOS FEM analysis

SHELL4 ELEMENTS

2x2	free-free	113	143	184	232	232
	supported	213	444	444	662	662
	clamped	315	450	450	882	882
4x4	free-free	147	195	255	346	346
	supported	235	569	569	853	1038
	clamped	416	795	795	1064	1184
8x8	free-free	157	222	285	397	397
	supported	239	594	594	939	1179
	clamped	433	875	875	1267	1550
40x40	free-free	160	234	296	416	416
	supported	240	599	599	958	1197
	clamped	437	891	891	1312	1595

SHELL8 ELEMENTS

2x2	free-free	160	206	300	323	323
	supported	214	520	520	929	4726
	clamped	516	832	832	4122	4726
4x4	free-free	160	233	298	410	410
	clamped	516	832	832	4122	4726
	supported	235	589	589	917	1170
8x8	free-free	434	884	884	1266	1657
	supported	159	234	296	412	412
	clamped	237	592	592	939	1180
20x20	free-free	434	880	880	1287	1564
	supported	159	234	296	412	412
	clamped	237	593	593	942	1182
	free-free	435	881	881	1291	1566

SHELL9 ELEMENTS

2X2	free-free	161	235	308	403	403
	supported	228	567	567	772	1602
	clamped	458	1024	1024	1311	5924
4X4	free-free	159	234	297	412	412
	supported	236	595	595	943	1204
	clamped	434	892	892	1301	1717
8X8	free-free	159	234	296	412	412
	supported	237	593	593	942	1184
	clamped	434	881	881	1291	1571
20X20	free-free	159	234	296	412	412
	supported	237	593	593	942	1183
	clamped	435	881	881	1292	1567

Note 1, Linda Turner, 09/03/99 11:29:53 AM
LIGO-T960213-A-D